blood advances

American Society of Hematology
2021 L Street NW, Suite 900,
Washington, DC 20036
Phone: 202-776-0544 | Fax 202-776-0545
bloodadvances@hematology.org

Physioxia improves the selectivity of hematopoietic stem cell expansion cultures

Tracking no: ADV-2023-009668R1

Kyomi Igarashi (Stanford University School of Medicine, United States) Iwo Kucinski (University of Cambridge, United Kingdom) Yan Yi Chan (Stanford University School of Medicine, United States) Tze-Kai Tan (Stanford University School of Medicine, United States) Hwei Minn Khoo (University of Oxford, United Kingdom) David Kealy (University of York, United Kingdom) Joydeep Bhadury (Stanford University School of Medicine, United States) Ian Hsu (Weatherall Institute of Molecular Medicine, United Kingdom) Pui Yan Ho (Stanford University, United States) Kouta Niizuma (University of Tsukuba,) John Hickey (Stanford University School of Medicine, United States) Garry Nolan (Stanford University, United States) Katherine Bridge (University of York, United Kingdom) Agnieszka Czechowicz (Stanford University School of Medicine, United States) Berthold Gottgens (University of Cambridge, United Kingdom) Hiromitsu Nakauchi (University of Tokyo, Japan) Adam Wilkinson (University of Oxford, United Kingdom)

Abstract:
Hematopoietic stem cells (HSCs) are a rare hematopoietic cell type that can entirely reconstitute the blood and immune systems following transplantation. Allogeneic HSC transplantation (HSCT) is used clinically as a curative therapy for a range of hematolymphoid diseases, but remains a high-risk therapy due to potential side effects including poor graft function and graft-vs-host disease (GvHD). Ex vivo HSC expansion has been suggested as an approach to improve hematopoietic reconstitution from low-cell dose grafts. Here, we demonstrate that we can improve the selectivity of polyvinyl alcohol (PVA)-based mouse HSC cultures through the use of physioxic culture conditions. Single-cell transcriptomic analysis confirmed inhibition of lineage-committed progenitor cells in physioxic cultures. Long-term physioxic expansion also afforded culture-based ex vivo HSC selection from whole bone marrow, spleen, and embryonic tissues. Furthermore, we provide evidence that HSC-selective ex vivo cultures deplete GvHD-causing T cells and that this approach can be combined with genotoxic-free antibody-based conditioning HSCT approaches. Our results offer a simple approach to improve PVA-based HSC cultures and the underlying molecular phenotype, as well as highlight the potential translational implications of selective HSC expansion systems for allogeneic HSCT.

Conflict of interest: COI declared - see note

COI notes: HN is a co-founder and shareholder in Megakaryon, and Century Therapeutics. ACW is a consultant for Graphite Bio and ImmuneBridge. AC discloses financial interests in the following entities working in the rare genetic disease space: Beam Therapeutics, Decibel Therapeutics, Editas Medicines, Global Blood Therapeutics, GV, Lyrik Therapeutics, Magenta Therapeutics, and Spotlight Therapeutics. However, none of these companies had input into the design, execution, interpretation, or publication of the work in this manuscript.

Preprint server: No;

Author contributions and disclosures: KJI, IK, SC, DK, TKT, JB, IH, PYH, HMK, JWH, and KN designed experiments, performed experiments, analyzed the data, and reviewed and edited the manuscript. GPN, KB, AC, BG, and HN designed experiments, analyzed the data and reviewed and edited the manuscript. ACW designed experiments, performed experiments, analyzed the data, and wrote the manuscript.

Non-author contributions and disclosures: No;

Agreement to Share Publication-Related Data and Data Sharing Statement: A single cell RNA-seq website resource is available here: http://128.232.227.172/Igarashi2022/ (username: BGlab; password: RHQoz89jc). Raw and processed data are available on GEO (GSE207743, GSE175400, GSE207740).

Clinical trial registration information (if any):

Physioxia improves the selectivity of hematopoietic stem cell expansion cultures

SHORT TITLE:
Selective blood stem cell cultures via physioxia

AUTHORS:
Kyomi J. Igarashi[1,2,*], Iwo Kucinski[3,*], Yan Yi Chan[1,4], Tze-Kai Tan[5,6], Hwei Minn Khoo[7], David Kealy[8], Joydeep Bhadury[1,2], Ian Hsu[7], Pui Yan Ho[1,4], Kouta Niizuma[1,2], John W. Hickey[5,6], Garry P. Nolan[5,6], Katherine S. Bridge[8], Agnieszka Czechowicz[1,4], Berthold Gottgens[3], Hiromitsu Nakauchi[1,2,9], Adam C. Wilkinson[1,7,†]

AFFILIATIONS:
[1]Institute for Stem Cell Biology and Regenerative Medicine, Stanford University School of Medicine, Lorry I. Lokey Stem Cell Research Building, 265 Campus Drive, Stanford, CA, USA
[2]Department of Genetics, Stanford University School of Medicine, Stanford, CA, USA
[3]Wellcome-MRC Cambridge Stem Cell Institute, Department of Haematology, Jeffrey Cheah Biomedical Centre, University of Cambridge, Cambridge, UK
[4]Department of Pediatrics, Stanford University School of Medicine, Stanford, CA, USA
[5]Department of Microbiology and Immunology, Stanford University School of Medicine, Stanford University, Stanford, CA, USA
[6]Department of Pathology, Stanford University School of Medicine, Stanford University, Stanford, CA, USA
[7]MRC Weatherall Institute of Molecular Medicine, University of Oxford, Oxford, UK
[8]York Biomedical Research Institute, Department of Biology, University of York, UK.
[9]Division of Stem Cell Therapy, Distinguished Professor Unit, The Institute of Medical Science, The University of Tokyo, Tokyo, Japan
*Co-first authors
†Corresponding author: adam.wilkinson@imm.ox.ac.uk

ABSTRACT:

Hematopoietic stem cells (HSCs) are a rare hematopoietic cell type that can entirely reconstitute the blood and immune systems following transplantation. Allogeneic HSC transplantation (HSCT) is used clinically as a curative therapy for a range of hematolymphoid diseases, but remains a high-risk therapy due to potential side effects including poor graft function and graft-vs-host disease (GvHD). Ex vivo HSC expansion has been suggested as an approach to improve hematopoietic reconstitution from low-cell dose grafts. Here, we demonstrate that we can improve the selectivity of polyvinyl alcohol (PVA)-based mouse HSC cultures through the use of physioxic culture conditions. Single-cell transcriptomic analysis confirmed inhibition of lineage-committed progenitor cells in physioxic cultures. Long-term physioxic expansion also afforded culture-based ex vivo HSC selection from whole bone marrow, spleen, and embryonic tissues. Furthermore, we provide evidence that HSC-selective ex vivo cultures deplete GvHD-causing T cells and that this approach can be combined with genotoxic-free antibody-based conditioning HSCT approaches. Our results offer a simple approach to improve PVA-based HSC cultures and the underlying molecular phenotype, as well as highlight the potential translational implications of selective HSC expansion systems for allogeneic HSCT.

KEY POINTS:

- Physioxia improves the selectivity of polyvinyl alcohol-based mouse hematopoietic stem cell cultures
- Selective hematopoietic stem cell cultures deplete graft-vs-host disease causing T cells

INTRODUCTION:

Self-renewing multipotent hematopoietic stem cells (HSCs) support the blood and immune systems throughout life[1-3]. HSCs first arise in the mouse embryo around E10.5 and initially localize to the fetal liver before moving to the bone marrow around the time of birth[4]. While the bone marrow microenvironment is the most studied HSC niche, HSCs have also been described in other organs such as the spleen[5,6]. HSCs are usually very rare, at an estimated frequency of ~1:30,000 cells within the adult bone marrow, and just ~1:300,000 in the adult spleen[7]. This has hindered efforts to characterize this biologically interesting stem cell population.

The transplantation of healthy HSCs into a patient (termed HSCT) is a potentially curative therapy for a wide range of blood diseases[8]. However, although HSCT has been used for over 60 years, this therapy often still remains a treatment of last resort due to several safety concerns[9,10]. First, allogeneic HSCT currently requires patients to undergo genotoxic pre-conditioning via radiation therapy and/or chemotherapy to enhance donor engraftment and prevent rejection. Second, donor and recipient must be sufficiently immune-matched to avoid graft-vs-host disease (GvHD), which is caused by allo-reactive T cells that contaminate the donor HSC graft. GvHD represents a serious potential side effect of HSCT and the donor-recipient immune-matching requirement to avoid it also limits the number of potential donors for a transplant. An ideal HSCT paradigm would involve availability of large numbers of HSCs so that toxic chemo-irradiative pre-conditioning would not be required and cell products that lack GvHD-inducing T cells to improve donor-recipient immune compatibility.

The biological and clinical importance of HSCs has driven wide efforts to sustain HSCs ex vivo[11,12]. However, for a long time, stable expansion of HSCs has remained a major challenge for the field. We recently discovered that polymer-based media could support long-term ex vivo expansion of functional mouse HSCs[13,14]. While these cultures were initiated from FACS-purified $CD150^{+}CD34^{-/lo}$c-$Kit^{+}Sca1^{+}Lineage^{-}$ ($CD150^{+}CD34^{-/lo}$KSL) HSCs, a range of c-$Kit^{+}Sca1^{-}Lineage^{-}$ progenitor cells built up in these cultures over time, reducing HSC purity. Here, we describe that through optimizing O_2 concentrations for ex vivo HSC cultures, we could limit the buildup of progenitors and mature hematopoietic cells within long-term polyvinyl alcohol (PVA)-based cultures and thereby improve HSC culture selectivity. These optimized culture conditions selectively expand HSCs from whole bone marrow cells (WBMCs) and whole spleen cells, while depleting mature hematopoietic cells including T cells. Depletion of allo-reactive T cells was demonstrated by transplantation of allogeneic cells, which confirmed that HSC-selective cultures prevented acute GvHD. Finally, we present evidence that these methods can be combined with antibody-mediated inhibition of graft rejection to achieve HSCT without genotoxic-conditioning.

METHODS:

Mice

All animal experiments were approved by the Administrative Panel on Laboratory Animal Care at Stanford University or performed in accordance with UK Home Office regulations. C57BL/6-CD45.2 mice (000664), C57BL/6-CD45.1 mice (PepboyJ; 002014), and Balb/c mice (000651) were purchased from the Jackson Laboratory or bred at the University of Oxford. C57BL/6-CD45.1/CD45.2 mice were bred from C57BL/6-CD45.1 and C57BL/6-CD45.2 at Stanford University. Fancd2$^{-/-}$ mice[15] were generously provided by Ken Weinberg and bred at Stanford University. All mice were 8-12 weeks at the experiment start point.

Purified HSC cultures

Immunophenotypic CD150^{+}CD34$^{-/lo}$c-Kit^{+}Sca1^{+}Lineage^{-} HSCs were isolated from pelvic, femur, tibia, and vertebrae from C57BL/6-CD45.1 or C57BL/6-CD45.2 mice using an AriaII cell sorter (BD and cultured as described previously[14]. Cells were incubated at 5% CO_2 and indicated O_2 levels using a multigas incubator (ThermoFisher HERACell 150i or PHC MCO-170M-PE Incusafe), with complete media changes (performed in regular tissue culture hoods) every 2-3 days after the initial 5 days. See Supplementary Information for further details.

Unfractionated bone marrow and spleen cultures

Unfractionated whole bone marrow or whole spleen were strained with a 100um filter and then plated on CellBIND (Corning) plates in HSC media (see composition above) and incubated at 5% CO_2 and indicated O_2 levels, with complete media changes every 2-3 days.

Cytometric analyses

Flow cytometry and cytometry by time of flight (CyTOF) were performed at indicated timepoints. Cells were antibody stained (CD201-APC, cKit-BV421, Sca1-PE, Gr1-APC/eFluor780, Ter119-APC/eFluor780, CD4-APC/eFluor780, CD8-APC/eFluor780, CD45R-APC/eFluor780, CD127-APC/eFluor780) for 30 minutes at 4°C, washed and then analyzed using a LSRFortessa (BD) using PI as a live/dead cell stain. CyTOF was performed as detailed in the Supplementary Information.

Transplantation assays

For competitive transplantation assays, 5000 day-28 culture cells derived from C57BL/6-CD45.1 mice were transplanted alongside 1x10^{6} C57BL/6-CD45.1/CD45.2 competitor whole bone marrow cells (WBMCs) into 10Gy lethally irradiated C57BL/6-CD45.2 recipient mice. Secondary transplantation assays were performed as above but using 2x10^{6} WBMCs isolated from primary recipients. For allogeneic transplantation assays into Balb/c mice, fresh or day-28 cultured cells derived from WBMCs and/or whole spleen cells isolated from C57BL/6-CD45.1 mice were transplanted into 7Gy irradiated Balb/c mice. Hematoxylin and eosin staining was performed on paraformaldehyde-fixed livers by the Stanford Animal Histology Service. For minor allele mismatch transplantation assays into Fancd2$^{-/-}$ mice, day-28 cultured cells derived from WBMCs or CD150^{+}CD48^{-}KSL HSCs, or fresh CD150^{+}CD48^{-}KSL HSCs isolated from

C57BL/6-CD45.1 mice were transplanted into Fancd2$^{-/-}$ mice. Where indicated, mice were pre-treated with 500ug of anti-CD4 (GK1.5; BioXCell) 7-days before transplantation.

RNA-seq analyses

For bulk RNA-seq day-28 cultured cells were stained as indicated above and CD201^{+}CD150^{+}c-Kit^{+}Sca1^{+}Lineage^{-} and Kit^{+}Sca1^{-}Lineage^{-} cells FACS isolated and RNA extracted using a QIAGEN RNeasy micro kit. RNA-seq was performed by Novogene. Single cell (sc)RNA-seq was performed using 10X Genomics v3 reagents, as detailed in the Supplementary Information.

A single cell RNA-seq website resource is available here: http://128.232.227.172/Igarashi2022/ (username: BGlab; password: RHQoz89jc). Raw and processed data are available on GEO (GSE207743, GSE175400, GSE207740).

RESULTS:

Physiological O_2 concentrations reduce differentiation in long-term ex vivo HSC cultures

The importance of O_2 concentration in cell culture conditions has come to the forefront in discussions around improving the physiological relevance and translational capacity of basic biological findings from ex vivo studies[16-18]. Recapitulating the pericellular oxygen partial pressure (pO_2) found in specific tissue microenvironments has demonstrated significant value in producing data which is both more representative of in vivo physiology and more experimentally robust[19]. Direct measurement of pO_2 in the bone marrow of mice has identified a range of 9.9-32 mm Hg O2 (1.3-4.2%)[20], of which LT-HSCs are not found in bone marrow niches with the deepest hypoxia, but rather reside in pO_2 of 18-19 mm Hg (2-3%)[21]. We hypothesized that calibration of O_2 concentration to levels more representative of the bone marrow might further improve our HSC cultures. In our previous studies, HSCs were grown in standard 20% O_2 tissue culture incubators, which yields a pericellular O_2 concentration of ~18.4%[21-23]. We compared these HSC culture conditions with cultures grown at 5% O_2, and 1% O_2 (pericellular O_2 concentrations of ~3.5% and ~0.7%, respectively) (**Figure 1A**). Flow cytometry after 4-week culture identified striking differences in culture composition with significant increases in the frequency of phenotypic CD201^{+}CD150^{+}KSL populations (**Figure 1A-B**), which has recently been proposed as the ex vivo HSC fraction[24-26]. This high frequency of CD201^{+}CD150^{+}KSL cells was largely stable at 30-40% of live cells at low O_2 throughout the 4-week culture (**Figure 1B**).

In terms of absolute cell numbers per well, 1% and 5% O_2 reduced the number of live cells by ~50% (**Figure 1C**), meaning that similar numbers of CD201^{+}CD150^{+}KSL cells were generated in all cultures (**Figure 1D**). The increased frequency of CD201^{+}CD150^{+}KSL cells was driven by a decrease in non-KSL cells at low O_2 (**Figure 1E**). Competitive transplantation assays confirmed the functional capacity of the cells cultured at all O_2 concentrations. Compared to 20% O_2 cultured cells, 5% O_2 cultures displayed ~2-fold higher donor chimerism by the 16-week

endpoint (**Figure 1F, S1A**). By contrast, 1% O_2 cultured cells initially displayed similar chimerism to 5% O_2 cultures at 4-weeks, but dropped down to levels similar to 20% O_2 cultures by 16 weeks (**Figure 1F, S1A**). The cause of this lower engraftment rate at 1% O_2 is unclear.

To characterise the molecular consequences of low O_2 culture conditions on HSC expansion, we performed RNA-sequencing (RNA-seq) analysis on $CD201^+CD150^+KSL$ cells from 4-week cultures. The $c\text{-}Kit^+Sca1^-Lineage^-$ cells were also analyzed from the 20% O_2 cultures. Initial principal component analysis (PCA) separated $CD201^+CD150^+KSL$ samples from $c\text{-}Kit^+Sca1^-Lineage^-$ samples via PC1 while 20% O_2 $CD201^+CD150^+KSL$ samples separated from 5% and 1% $CD201^+CD150^+KSL$ samples via PC2 (**Figure S1B**). When compared against the $c\text{-}Kit^+Sca1^-Lineage^-$ samples, gene set enrichment analysis (GSEA) identified enrichment for LT-HSC gene sets in the $CD201^+CD150^+KSL$ cell samples for all O_2 concentrations, while the $c\text{-}Kit^+Sca1^-Lineage^-$ samples were enriched for progenitor gene sets (**Figure S1C**). These results confirmed $CD201^+CD150^+KSL$ cells as phenotypic (p)HSCs and $c\text{-}Kit^+Sca1^-Lineage^-$ cells as phenotypic hematopoietic progenitor cells (pHPCs).

To investigate the transcriptional differences between these samples, we performed differential gene expression analysis. Between 5% and 1% O_2 pHSC samples, few differentially expressed genes were observed (**Figure 1G**). By contrast, large gene expression differences were observed between 20% and 5% O_2 pHSCs (**Figure 1G**). GO term analysis identified upregulation of transcriptional and endoplasmic reticulum stress pathways in 20% O_2 pHSCs (**Figure 1H**), which corresponded to the observed differential expression of the stress response factor *Atf5* (**Figure 1G**). Stress response pathway activity is known to induce HSC differentiation[27,28], which may explain why 20% O_2 HSC cultures contained more differentiated cell types. Amino acid transporters were also enriched in 20% pHSCs (relative to 5% O_2 pHSCs), while sterol and cholesterol metabolism pathways were dominant among upregulated genes at 5% and 1% O_2 (relative to 20% O_2 pHSCs) (**Figure 1H**).

To search for pathways that could be playing a role in the selectivity for $CD201^+CD150^+KSL$ in the low O_2 cultures, we screened 116 small molecule inhibitors targeting various intracellular pathways (see **Table S1** for details) using 21-day expanded cells at 20% O_2. One of the top hits was IACS-010759, an inhibitor of mitochondrial complex I, which plays an important role in aerobic respiration (**Figure 1I**). We next tested this compound on fresh HSCs. At 20% O_2, we observed significant increases in $CD201^+CD150^+KSL$ frequencies, and similar reductions in total cell numbers and non-KSL cells as our low O_2 cultures using 20 nM (**Figure 1J**). By contrast, little difference was seen when IACS-010759 was added to 5% O_2 or 1% O_2 HSC cultures. These results suggest that reduced mitochondrial respiratory chain activity may contribute to the inhibition of progenitor cells at low O_2. However, further studies are warranted to assess the metabolic state and dependencies of HSCs and progenitor cells in these culture conditions.

Low O_2 alters cellular heterogeneity within HSC cultures

To further investigate the altered cellular heterogeneity within these HSC cultures, we performed single-cell (sc)RNA-seq on 4-week cultured 20% O_2, 5% O_2, and 1% O_2 cultures derived from LT-HSCs as well as a fresh c-Kit-enriched bone marrow sample (**Figure 2A**). Batch correction using Harmony was performed to integrate fresh and cultured scRNA-seq profiles, since matching populations between samples were highly divergent with clear changes in expression (**Figure S2A**). The combined data revealed matching lineage topology and differentiation stages between fresh and cultured cells (**Figure S2B**) and identified 21 cell clusters (**Figure 2B**). We performed manual annotation based on established lineage markers[29], which highlighted differentiation trajectories towards monocytes, neutrophils, basophils/mast cells, megakaryocytes, erythroid and lymphoid/B cells (**Figure 2C, S3A**). To pinpoint the location of putative HSCs, we analyzed expression of known HSC markers (*Procr*, *Mecom*, *Mllt3*, *Ly6a*, *Hlf*) (**Figure S3A**) and HSC gene signatures (HSCscore[30] and RepopSig[24]) (**Figure S3B-C**), which showed the highest values within the cluster 1. Comparing cluster frequency for each sample, we observed striking differences in abundance between the high (20%) and low (5% and 1%) O_2 cultures, whereas the 5% and 1% patterns were broadly similar (**Figure 2D, S3D**). Specifically, we identified increased abundance of low O_2 cultured cells in the HSC and intermediate progenitor clusters accompanied by relative depletion of the more differentiated clusters (**Figure 2E**). Cells with the highest RepopSig score were also much more abundant at low O_2 levels (**Figure S3E**).

To probe the apparent block in differentiation caused by low O_2, we used estimated pseudotime and the CellRank framework to infer cell fate probabilities for the main differentiation trajectories (**Figure 2F-G, S4A**). At low O_2 levels, cell density along pseudotime confirmed a sharp reduction in cell number at around the 0.02-0.021 pseudotime mark for both megakaryocyte and neutrophil trajectories (arrows in **Figures 2H** and **S4B**). At this stage, we observed almost no fate separation between the basophil, erythroid and megakaryocyte trajectories (**Figure S4C-D**), while the neutrophil trajectory had just separated from the other fates (**Figure S4E**). Thus, we asked which genes were dynamically expressed around the differentiation stage with the clear drop in cell numbers for the neutrophil and megakaryocyte trajectories.

For the megakaryocyte trajectory, we identified 75 differentially expressed genes, which showed stereotypic pattern and order of gene expression changes (**Figure 2I**). Many of these were known hematopoietic regulators[31]. For instance, several HSC-associated genes (e.g., *Mecom*, *Hlf*, *Ly6a*) dropped off early on (by pseudotime value 0.015). On the other hand, a different set of genes including several known markers of differentiation (e.g., *Gata1*, *Gata2*, *Ms4a2*, *Ms4a3*) were beginning to be upregulated around the putative differentiation block stage.

The dynamic genes in the neutrophil trajectory showed a limited overlap with the megakaryocyte trajectory, although we observed a similar decrease in *Mecom* expression in both (**Figure S4F**). Instead, the list of dynamic genes featured genes associated with very early stage of myeloid differentiation, including *Mpo*, *Ctsg* and chemokine *Ccl9* appearing just before the region of interest and more typical neutrophil markers including *Elane*, *Cebpe* appearing later (**Figure S4F**). Together, these results pinpoint critical stages in the transition from the HSC-like state to more differentiated progenitors that are suppressed in low O_2 cultures, and suggest specific molecular events associated with this transition.

Finally, we performed differential gene expression analysis to interrogate O_2 concentration specific-transcriptomes specifically within our cluster 1 HSCs. We identified upregulation of the interferon response specifically at 5% O_2 (**Figure 2J, S4G**). This higher inflammatory signaling could relate to the recently described link between inflammatory signaling and ex vivo HSC self-renewal[32]. To allow for the community to interrogate these datasets, we have generated a website portal for interrogating gene expression within these clusters (http://128.232.227.172/Igarashi2022/).

Low O_2 affords HSC expansion from unfractionated hematopoietic cell populations

The selectivity of these low O_2 cultures prompted us to consider whether culture-based enrichment of HSCs could be achieved from WBMCs (**Figure 3A**). While we have previously succeeded in expanding LT-HSCs from c-Kit$^+$ hematopoietic stem and progenitor cells (HSPCs), LT-HSC selection from WBMCs was not possible at 20% O_2[33]. Compared to 20% O_2 WBMC cultures, similar number of live cells were generated after four weeks at 5% O_2, but lower numbers were generated at 1% O_2 (**Figure 3B**). Both 5% O_2 and 1% O_2 cultures contained ~3-fold more CD201$^+$CD150$^+$KSL cells than the 20% O_2 cultures (**Figure 3C, S5A**). In primary competitive transplantation assays, 5% O_2 and 1% O_2 cultured cells performed better than 20% O_2 cultures (**Figure 3D, S5B**). However, only 5% O_2 cultures achieved robust multilineage PB chimerism in secondary recipients (**Figure 3E, S5C**).

To track the cellular heterogeneity within these WBMC cultures over time, we performed cytometry by time of flight (CyTOF) analysis using a hematopoiesis antibody panel (**Figure 3F**; **Table S2**). Given the superior functional results at 5% O_2, we focused our analysis on this culture condition. We used unsupervised clustering to resolve cell populations within the cultures, and manually annotated these immunophenotypic clusters (**Figure S5D**). Clusters at less than 1% of the cell cultures were grouped as "Other". Over the first week, the CD201$^+$KSL fraction was initially very rare (0.5%), but increased after day 7 and reached over 50% by day 28 (**Figure 1F**). The inverse was seen for granulocytes/monocytes and erythroid cells, which were initially high and dropped down between day 7 and 14.

To assess a second hematopoietic cell population, we also evaluated whole spleen cells in 5% O_2 culture using this CyTOF time course assay (**Figure 3G, S5A**). Similar to WBMC cultures, $CD201^+$KSL frequencies were initially very low and rose between day 7 and day 14, while erythroid cells displayed the inverse. In fresh spleen, $CD4^+$ and $CD8^+$ T cells were initially present at a frequency of 27% and were gradually depleted over time in culture. By day 28, T cells were just 2% of the culture. Compared with the WBMC cultures, lower $CD201^+$KSL frequencies were observed in spleen cultures at day 28 (23% vs 50%; **Figure 3F-G**).

Within both the WBMC and whole spleen cell cultures, we could identify two KSL compartments, one marked by CD201 ($CD201^+$KSL) and a second marked by CD41 ($CD41^+$KSL) (**Figure 3F-G, S5D**). Interestingly, while the $CD201^+$KSL expanded progressively over 28 days, the $CD41^+$KSL was most abundant at day 14 and 21 before dropping down at day 28. Further interrogation of the $Kit^+Sca1^+Lineage^-$ population specifically on day 28 suggested the major population (expressing $CD201^+$), also co-expressed CD31 (Pecam) and low levels of CD11b (Mac1) (**Figure S5E**). This analysis suggests additional markers that may help to resolve the HSC compartment ex vivo.

Given the selectivity of these culture conditions, we wondered whether we could use this system to assay for HSC expansion capacity. We therefore turned to embryonic development, to assay when expandable potential could be first observed. As definitive HSCs are reported to be first seen from embryonic day (E)10.5[4], we evaluated expansion potential from various embryonic organs at E11.5 to E16.5 (**Figures 3H**). Our results largely mirrored the reported localization of HSCs in the developing embryo, with pHSCs expanding from the fetal liver from E13.5 onwards but were not observed from the yolk sac[34] (**Figure 3I**). Consistent with the reported transient HSC activity in the placenta[35,36], pHSCs expanded from E12.5 and E13.5 placenta, but not at later timepoints. Total live cell numbers (**Figure S5F**) also correlated with pHSCs presence in these cultures (**Figure 3I**), demonstrating culture selectivity. However, we did not detect expansion potential from the embryo at E11.5-12.5, suggesting our assay is selective for a subset of mature HSCs. These results suggest that this culture system may provide a useful assay for HSC expansion potential, although further work is needed to functionally validate these findings.

Ex vivo selective culture depletes GvHD-causing T cells

In allogeneic HSCT, allo-reactive T cells are a major cause of GvHD. Based on the robust concomitant depletion of T cells and expansion of HSCs in our whole spleen cell cultures, we hypothesized that our low O_2 ex vivo HSC expansion culture conditions would allow for engraftment post-allogeneic transplantation while avoiding GvHD. We therefore tested this in an acute GvHD model, where C57BL/6 donor cells were transplanted into irradiated allogeneic Balb/c recipients (**Figure 4A**). To induce acute GvHD in this model, a mixture of WBMCs and whole spleen cells were co-transplanted into irradiated recipients. Consistent with other reports[37], transplantation of fresh spleen/WBMC led to acute GvHD in 2 weeks (**Figure 4B, S6A**). By

contrast, recipients of cultured spleen/WBMCs, or even expanded spleen only survived long-term (**Figure 4B-C**) and displayed multilineage donor peripheral blood chimerism (**Figure S6B**). We further confirmed that the loss of T cells was responsible for the survival of these recipients by transplantation of fresh T cells with cultured spleen/WBMCs. Addition of fresh T cells led to rapid GvHD (**Figure S6C**). Together, these results confirm that low O_2 HSC-selective media conditions lead to depletion of mature immune cells and enrichment of transplantable HSPCs.

Finally, we evaluated whether we could combine this GvHD-free HSC expansion method with antibody-based inhibition of immune rejection in a relevant allogenic HSCT mouse model (**Figure 4D**). Given the toxicities of bone marrow conditioning regimens and GvHD in Fanconi Anemia patients receiving allogeneic HSC transplantation, we selected a minor allele mismatch Fancd2$^{-/-}$ HSCT mouse model for this proof-of-concept study. Minor mismatches between wildtype C57BL/6 and Fancd2$^{-/-}$ mice lead to rejection of C57BL/6 donor cells when transplanted without conditioning[38]. However, the immune rejection can be inhibited with anti-CD4 antibody-based conditioning. We initially confirmed that anti-CD4 antibody treatment was necessary for engraftment of C57BL/6 cells (expanded from 5x10^6 WBMCs) in Fancd2$^{-/-}$ mice (**Figure S6D**). This experiment confirmed donor chimerism was dependent on anti-CD4-conditioning, but only achieved ~50% donor chimerism.

We repeated the transplantation experiments using cells expanded from 20x10^6 WBMCs in anti-CD4-conditioned Fancd2$^{-/-}$ mice. We achieved robust levels (>80%) of myeloid donor chimerism even within four weeks, which remained stably high over 20 weeks (**Figure 4E-F**). Notably, we observed lower levels of donor chimerism in the bone marrow HSC compartment than downstream progenitor and peripheral blood compartments. These results suggest a selective advantage in the ability of wild-type HSCs to support hematopoiesis, as compared to Fancd2$^{-/-}$ HSCs, and correspond with the reported reduced fitness of Fancd2$^{-/-}$ HSCs[38]. By contrast, 5000 freshly purified HSCs failed to engraft in Fancd2$^{-/-}$ mice while 4-week expanded cultures derived from 500 HSCs also displayed robust donor chimerism (**Figure 4E-F**). It is currently unclear why freshly-purified HSCs failed to engraft, but it is likely due to the low efficiency of engraftment in the non-conditioned setting and the need for supraphysiological HSC numbers for engraftment without bone marrow conditioning[39]. Together, these results highlight the potential translational implications for selective HSC expansion cultures.

DISCUSSION:

In this report, we demonstrate that we can improve the selectivity of PVA-based mouse HSC expansion cultures by optimizing O_2 concentrations. Furthermore, we have discovered that HSCs expand at the expense of GvHD-causing T cells under optimized low O_2 conditions. Additionally, we show proof-of-concept data for the combined use of expanded HSCs and antibody-mediated inhibition of immunologic rejection for allogeneic HSCT. However, further work will be needed to determine the translational potential of this work. For example, we will

need to investigate whether antibody conditioning for HLA-mismatched allo-HSCT could be combined with these approaches[40]. Additionally, our acute GvHD assays used T-cell-containing splenocytes, while peripheral blood products are used in the clinical setting.

The risks of GvHD that are associated with allo-HSCT have led to a major research effort in autologous HSCT gene therapies, where a patient's HSCs are collected, gene corrected, and then returned to reconstitute a healthy hematopoietic system[41,42]. However, this therapeutic strategy is still challenging, expensive, and patient access is usually limited to a few specialized centers. Our results suggest that if HSC selective expansion methods can be translated to humans and the risk of GvHD becomes avoidable, GvHD-free allogeneic HSCT could provide a competitive approach to autologous HSCT gene therapies. These results also highlight the potential caveats for allogeneic HSCT. In hematological malignancies, allo-T cell-mediated graft-vs-tumor effects are essential for long-term remission following HSCT[43]. However, expanded HSC products could be combined with T cell add-back strategies and there may be advantages of being able to separate the dose of HSPCs from the dose of T cells.

Besides the translational implications of this work, we also hope that our findings will support further investigations into HSC biology and hematopoiesis. The long-term ex vivo HSC culture system provides a tractable ex vivo model system to study HSC self-renewal and lineage commitment. In summary, we have identified physioxia as optimal for PVA-based HSC expansion cultures and demonstrated that these methods are highly selective for HSCs over more mature hematopoietic cell types, with implications for both basic and translational stem cell biology.

ACKNOWLEDGEMENTS:

We thank the Stanford Stem Cell Institute FACS Core and WIMM Flow Cytometry Core for flow cytometry access, the Stanford Animal Histology Service for histology, and the CZ-Biohub for performing the next generation sequencing. ACW acknowledges supported from the Kay Kendall Leukaemia Fund, the MRC, the NIH (K99HL150218), the Leukemia and Lymphoma Society (3385-19), and the Edward P. Evans Foundation. HN was supported by the NIH (R01DK116944; R01HL147124), the Ludwig Foundation, the Stinehart-Reed Foundation, and the Japan Society of the Promotion of Science. KJI acknowledges support from a National Science Foundation Fellowship. TKT acknowledges support from National Science Scholarship, A*STAR, Singapore. JB acknowledges support from the Swedish Research Council and the Assar Gabrielsson Foundation (2017-0034). IK and BG were supported by the Wellcome Trust, CRUK and the MRC. JWH was supported by an NIH T32 Fellowship (T32CA196585) and an American Cancer Society - Roaring Fork Valley Postdoctoral Fellowship (PF-20-032-01-CSM).

AUTHORSHIP CONTRIBUTION:

KJI, IK, SC, DK, TKT, JB, IH, PYH, HMK, JWH, and KN designed experiments, performed experiments, analyzed the data, and reviewed and edited the manuscript. GPN, KB, AC, BG, and HN designed experiments, analyzed the data and reviewed and edited the manuscript. ACW designed experiments, performed experiments, analyzed the data, and wrote the manuscript.

CONFLICT OF INTEREST DISCLOSURES:

HN is a co-founder and shareholder in Megakaryon, and Century Therapeutics. ACW is a consultant for Graphite Bio and ImmuneBridge. AC discloses financial interests in the following entities working in the rare genetic disease space: Beam Therapeutics, Decibel Therapeutics, Editas Medicines, Global Blood Therapeutics, GV, Lyrik Therapeutics, Magenta Therapeutics, and Spotlight Therapeutics. However, none of these companies had input into the design, execution, interpretation, or publication of the work in this manuscript.

REFERENCES:

1. Wilkinson AC, Igarashi KJ, Nakauchi H. Haematopoietic stem cell self-renewal in vivo and ex vivo. *Nat Rev Genet*. 2020.
2. Eaves CJ. Hematopoietic stem cells: concepts, definitions, and the new reality. *Blood*. 2015;125(17):2605-2613.
3. Orkin SH, Zon LI. Hematopoiesis: An evolving paradigm for stem cell biology. *Cell*. 2008;132(4):631-644.
4. Dzierzak E, Speck NA. Of lineage and legacy: the development of mammalian hematopoietic stem cells. *Nat Immunol*. 2008;9(2):129-136.
5. Morrison SJ, Scadden DT. The bone marrow niche for haematopoietic stem cells. *Nature*. 2014;505(7483):327-334.
6. Pinho S, Frenette PS. Haematopoietic stem cell activity and interactions with the niche. *Nat Rev Mol Cell Biol*. 2019;20(5):303-320.
7. Morita Y, Iseki A, Okamura S, Suzuki S, Nakauchi H, Ema H. Functional characterization of hematopoietic stem cells in the spleen. *Exp Hematol*. 2011;39(3):351-359 e353.
8. Copelan EA. Hematopoietic stem-cell transplantation. *N Engl J Med*. 2006;354(17):1813-1826.
9. Chabannon C, Kuball J, Bondanza A, et al. Hematopoietic stem cell transplantation in its 60s: A platform for cellular therapies. *Sci Transl Med*. 2018;10(436).
10. Hill GR, Betts BC, Tkachev V, Kean LS, Blazar BR. Current Concepts and Advances in Graft-Versus-Host Disease Immunology. *Annu Rev Immunol*. 2021;39:19-49.
11. Wilkinson AC, Nakauchi H. Stabilizing hematopoietic stem cells in vitro. *Current Opinion in Genetics & Development*. 2020;64:1 - 5.
12. Kumar S, Geiger H. HSC Niche Biology and HSC Expansion Ex Vivo. *Trends Mol Med*. 2017;23(9):799-819.
13. Wilkinson AC, Ishida R, Kikuchi M, et al. Long-term ex vivo haematopoietic-stem-cell expansion allows nonconditioned transplantation. *Nature*. 2019;571(7763):117-121.
14. Wilkinson AC, Ishida R, Nakauchi H, Yamazaki S. Long-term ex vivo expansion of mouse hematopoietic stem cells. *Nat Protoc*. 2020;15(2):628-648.

15. Houghtaling S, Timmers C, Noll M, et al. Epithelial cancer in Fanconi anemia complementation group D2 (Fancd2) knockout mice. *Genes Dev*. 2003;17(16):2021-2035.
16. Mantel CR, O'Leary HA, Chitteti BR, et al. Enhancing Hematopoietic Stem Cell Transplantation Efficacy by Mitigating Oxygen Shock. *Cell*. 2015;161(7):1553-1565.
17. Kobayashi H, Morikawa T, Okinaga A, et al. Environmental Optimization Enables Maintenance of Quiescent Hematopoietic Stem Cells Ex Vivo. *Cell Rep*. 2019;28(1):145-158.e149.
18. Wilkinson AC, Yamazaki S. The hematopoietic stem cell diet. *Int J Hematol*. 2018.
19. Al-Ani A, Toms D, Kondro D, Thundathil J, Yu Y, Ungrin M. Oxygenation in cell culture: Critical parameters for reproducibility are routinely not reported. *PLoS One*. 2018;13(10):e0204269.
20. Spencer JA, Ferraro F, Roussakis E, et al. Direct measurement of local oxygen concentration in the bone marrow of live animals. *Nature*. 2014;508(7495):269-273.
21. Christodoulou C, Spencer JA, Yeh SA, et al. Live-animal imaging of native haematopoietic stem and progenitor cells. *Nature*. 2020;578(7794):278-283.
22. Pavlacky J, Polak J. Technical Feasibility and Physiological Relevance of Hypoxic Cell Culture Models. *Front Endocrinol (Lausanne)*. 2020;11:57.
23. Zhdanov AV, Ogurtsov VI, Taylor CT, Papkovsky DB. Monitoring of cell oxygenation and responses to metabolic stimulation by intracellular oxygen sensing technique. *Integr Biol (Camb)*. 2010;2(9):443-451.
24. Che JLC, Bode D, Kucinski I, et al. Identification and characterization of in vitro expanded hematopoietic stem cells. *EMBO Rep*. 2022:e55502.
25. Becker HJ, Ishida R, Wilkinson AC, et al. A Single Cell Cloning Platform for Gene Edited Functional Murine Hematopoietic Stem Cells. *bioRxiv*. 2022:2022.2003.2023.485423.
26. Zhang Q, Konturek-Ciesla A, Yuan O, Bryder D. Ex Vivo Expansion Potential of Murine Hematopoietic Stem Cells: A Rare Property Only Partially Predicted by Phenotype. *bioRxiv*. 2022:2022.2006.2020.496822.
27. van Galen P, Kreso A, Mbong N, et al. The unfolded protein response governs integrity of the haematopoietic stem-cell pool during stress. *Nature*. 2014;510(7504):268-272.
28. Kruta M, Sunshine MJ, Chua BA, et al. Hsf1 promotes hematopoietic stem cell fitness and proteostasis in response to ex vivo culture stress and aging. *Cell Stem Cell*. 2021;28(11):1950-1965 e1956.
29. Dahlin JS, Hamey FK, Pijuan-Sala B, et al. A single-cell hematopoietic landscape resolves 8 lineage trajectories and defects in Kit mutant mice. *Blood*. 2018;131(21):e1-e11.
30. Hamey FK, Gottgens B. Machine learning predicts putative hematopoietic stem cells within large single-cell transcriptomics data sets. *Exp Hematol*. 2019;78:11-20.
31. Wilkinson AC, Gottgens B. Transcriptional regulation of haematopoietic stem cells. *Adv Exp Med Biol*. 2013;786:187-212.
32. Chagraoui J, Lehnertz B, Girard S, et al. UM171 induces a homeostatic inflammatory-detoxification response supporting human HSC self-renewal. *PLoS One*. 2019;14(11):e0224900.
33. Ochi K, Morita M, Wilkinson AC, Iwama A, Yamazaki S. Non-conditioned bone marrow chimeric mouse generation using culture-based enrichment of hematopoietic stem and progenitor cells. *Nat Commun*. 2021;12(1):3568.
34. Ganuza M, Chabot A, Tang X, et al. Murine hematopoietic stem cell activity is derived from pre-circulation embryos but not yolk sacs. *Nat Commun*. 2018;9(1):5405.

35. Gekas C, Dieterlen-Lièvre F, Orkin SH, Mikkola HK. The placenta is a niche for hematopoietic stem cells. *Dev Cell*. 2005;8(3):365-375.
36. Ottersbach K, Dzierzak E. The murine placenta contains hematopoietic stem cells within the vascular labyrinth region. *Dev Cell*. 2005;8(3):377-387.
37. Schroeder MA, DiPersio JF. Mouse models of graft-versus-host disease: advances and limitations. *Dis Model Mech*. 2011;4(3):318-333.
38. Chandrakasan S, Jayavaradhan R, Ernst J, et al. KIT blockade is sufficient for donor hematopoietic stem cell engraftment in Fanconi anemia mice. *Blood*. 2017;129(8):1048-1052.
39. Shimoto M, Sugiyama T, Nagasawa T. Numerous niches for hematopoietic stem cells remain empty during homeostasis. *Blood*. 2017;129(15):2124-2131.
40. George BM, Kao KS, Kwon HS, et al. Antibody Conditioning Enables MHC-Mismatched Hematopoietic Stem Cell Transplants and Organ Graft Tolerance. *Cell Stem Cell*. 2019;25(2):185-192 e183.
41. Morgan RA, Gray D, Lomova A, Kohn DB. Hematopoietic Stem Cell Gene Therapy: Progress and Lessons Learned. *Cell Stem Cell*. 2017;21(5):574-590.
42. Dever DP, Porteus MH. The changing landscape of gene editing in hematopoietic stem cells: a step towards Cas9 clinical translation. *Curr Opin Hematol*. 2017;24(6):481-488.
43. Negrin RS. Graft-versus-host disease versus graft-versus-leukemia. *Hematology Am Soc Hematol Educ Program*. 2015;2015:225-230.

FIGURE LEGENDS:

Figure 1: Improved stability of PVA-based HSC cultures in low O_2

A. Schematic of low O_2 HSC cultures (left). Mouse $CD150^+CD34^-KSL$ HSCs were sorted into PVA-based media in 96-well plates (50 cells per well) in 200ul of media and cultured for four weeks at 20%, 5%, or 1% O_2. Representative flow cytometry plots for 4-week HSC-derived cultures (right). Upper panels display c-Kit and Sca1 expression within the $Lineage^-$ cell fraction while lower panels display CD201 and CD150 expression within the KSL cell fraction.

B. Mean frequency of $CD201^+CD150^+KSL$ cells within the HSC-derived cultures described in A. n=4.

C. Mean number of live cells per well within the HSC-derived cultures described in A. n=4.

D. Mean number of $CD201^+CD150^+KSL$ cells per well within the HSC-derived cultures described in A. n=4.

E. Mean number of non-KSL cells per well within the HSC-derived cultures described in A. n=4.

F. 16-week donor peripheral blood chimerism from 4-week-old HSC-derived cultures incubated at 20%, 5%, or 1% O_2. 5000 cells from each culture were transplanted alongside $1x10^6$ WBMCs into lethally irradiated recipients. Mean ± standard deviation (SD); n=8-9.

G. Differential gene expression analysis between 5% O_2 pHSC and 1% O_2 pHSC samples (left), or 5% O_2 pHSC and 20% O_2 pHSC samples (right). Results displayed as Log2(fold-change) vs -Log(adjusted P value).

H. GO term enrichment analysis for underexpressed and overexpressed genes between 5% O_2 pHSC and 20 % O_2 pHSC samples.

I. Fold change in $CD201^+CD150^+KSL$ cells relative to control wells following a 7-day culture with the indicated compounds at 20% O_2. Of 116 compounds tested, only the 74 that supported cell survival/growth are displayed (see **Supplementary Table 1** for a full list). Cell cultures were initiated with 50 $CD201^+CD150^+KSL$ cells resorted from 3-week HSC cultures. Mean of 4 wells (from 2 biological replicates) displayed.

J. Mean frequency of $CD201^+CD150^+KSL$ cells (left) and mean number of live cells per well (left), within 7-day HSC-derived cultures at 20% O_2, 5% O_2, or 1% O_2, cultured with either DMSO or the mitochondrial complex I inhibitor IACS-01-759 (20 nM). n=6.

Statistical analysis was performed by ANOVA. n.s. denotes not significant; * denotes $p<0.05$; **** denotes $p<0.0001$.

Figure 2: Single-cell transcriptomics identifies molecular consequences of low O_2 on HSC cultures

A. Schematic of the scRNA-seq experiment analyzing HSPCs cultured at different O_2 concentrations.

B. UMAP projections of all samples with color-coded cluster membership.

C. Manual annotation of clusters in B based on marker gene expression. Bas, basophil; Ery, erythroid; ILC, innate lymphoid cell; Ly/DC, lymphoid/dendritic cell; Meg, megakaryocyte; MC, mast cell; Mono typ, typical monocyte; Neu, neutrophil; prog, progenitor.

D. UMAP projections of all cells (grey) and cells from indicated conditions (blue). In each case, an equal cell number was randomly selected for each sample.
E. Bar plot indicating relative cell abundance in areas of the landscape for each sample. Areas were chosen as follows: HSC - cluster 1, Intermediate prog - clusters 0 and 2-4, Ery/Bas/MC/Meg prog - clusters 6, 7 and 17, Neu/Mono/DC - clusters 5, 11 and 14, Other - remaining clusters. * a indicates statistically significant change in cell abundance (FDR <0.05) compared to the 20% O_2 condition.
F. UMAP projection color-coded with diffusion pseudotime values, overlaid with arrows indicating putative paths of differentiation using random walks estimation with CellRank Pseudotime Kernel.
G. UMAP projection color-coded by cell fate probability of cells differentiating into the tip of cluster 17 (Megakaryocytes).
H. Cell density along the trajectory shown in G for each sample, only pseudotime values between 0 and 0.05 are shown. Vertical lines indicate the regions of interest, where cells at 5% and 1% O_2 disappear.
I. Heatmap of genes differentially expressed between the beginning and end of the region of interest shown in H.
J. Enrichr gene enrichment analysis of upregulated genes within cluster 1 at 5% O_2, compared to 20% (left), and 1% O_2 (right).

Figure 3: Low O_2 cultures expand HSCs from unfractionated WBMCs and embryonic tissues

A. Schematic of low O_2 WBMC cultures. Unfractionated mouse WBMCs were seeded into PVA-based media in 24-well plate wells ($5x10^6$ cells per well) in 1ml of media and cultured for four weeks at 20%, 5%, or 1% O_2.
B. Mean number of live cells per well within the WBMC-derived cultures described in A at day-28. n=6.
C. Mean number of $CD201^+CD150^+KSL$ cells per well within the WBMC-derived cultures described in A at day-28. n=6.
D. 16-week donor peripheral blood chimerism from 4-week-old WBMC-derived cultures incubated at 20%, 5%, or 1% O_2. 5000 cells from each culture were transplanted alongside $1x10^6$ WBMCs into lethally irradiated recipients. Mean ± SD; n=3-5.
E. 12-week donor peripheral blood chimerism following secondary transplantation of WBMCs from primary recipient mice described in D. Mean ± SD; n=3-4.
F. Schematic of CyTOF time course during 5% O_2 WBMC cultures (left) and frequency of immunophenotypic cell populations at indicated timepoints (right). See **Figure S5B** for cell immunophenotypes.
G. Schematic of CyTOF time course during 5% O_2 whole spleen cell cultures (left) and frequency of immunophenotypic cell populations over 28-day cultures (right). See **Figure S5B** for cell immunophenotypes.

H. Schematic of selective HSC expansion assay from mouse embryonic tissues.
I. Mean number of $CD201^+CD150^+KSL$ cells generated from E11.5-12.5 embryonic tissue (excluding extraembryonic tissues and fetal liver), E11.5-16.5 heart, yolk sac, placenta, and fetal liver-derived cultures. Starting cell number indicated in brackets seeded in 1ml of media. Statistical analysis was performed by ANOVA. n.s. denotes not significant; * denotes $p<0.05$; **denotes $p<0.01$; **** denotes $p<0.0001$.

Figure 4: Low O_2 selective HSC cultures avoid GvHD

A. Schematic of allogeneic transplantation assay. Unfractionated WBMCs and/or spleen cells from C57BL/6 mice were transplanted into irradiated Balb/c mice before or after 4-week PVA-based culture.
B. Survival of Balb/c recipients in the assay described in B, following transplantation of $5x10^6$ WBMCs and $5x10^6$ whole spleen cells (fresh or cultured) from C57BL/6 mice. n=7-8. Statistical analysis was performed by Mantel-Cox test. **** denotes $p<0.0001$.
C. Survival of Balb/c recipients in the assay described in B, following transplantation of $5x10^6$ whole spleen cells (fresh or cultured) from C57BL/6 mice. n=7-8. Statistical analysis was performed by Mantel-Cox test. **** denotes $p<0.0001$.
D. Schematic of antibody conditioning transplantation assay. 4-week cultured WBMCs (derived from $20x10^6$ WBMCs), 4-week cultured HSCs (derived from 500 HSCs), or 5000 fresh HSCs from C57BL/6-CD45.1 mice were transplanted into $Fancd2^{-/-}$-CD45.2 mice 7 days after treatment with anti-CD4 (GK1.5) antibody.
E. Donor chimerism in $Fancd2^{-/-}$ recipient mice at 4-20 weeks with peripheral blood $Mac1^+Gr1^+$ myeloid cells (top left panel), $B220^+$ B cells (top right panel), $CD4^+CD3^+$ T cells (bottom left panel), and $CD8^+CD3^+$ T cells (bottom right panel). n=4.
F. Donor chimerism in $Fancd2^{-/-}$ bone marrow and peripheral blood compartments for recipients described in F. n=4.

Figure 1

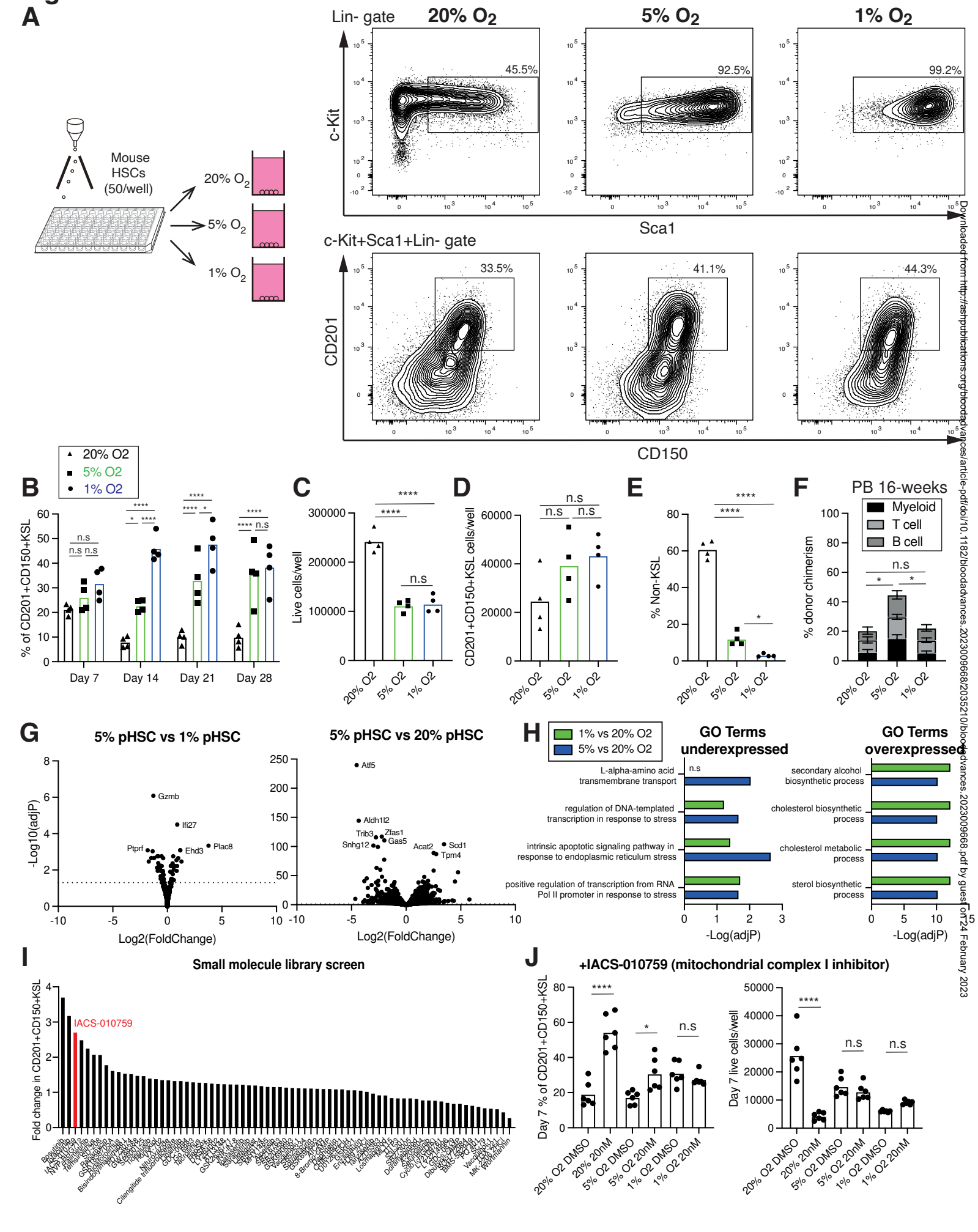

Figure 2

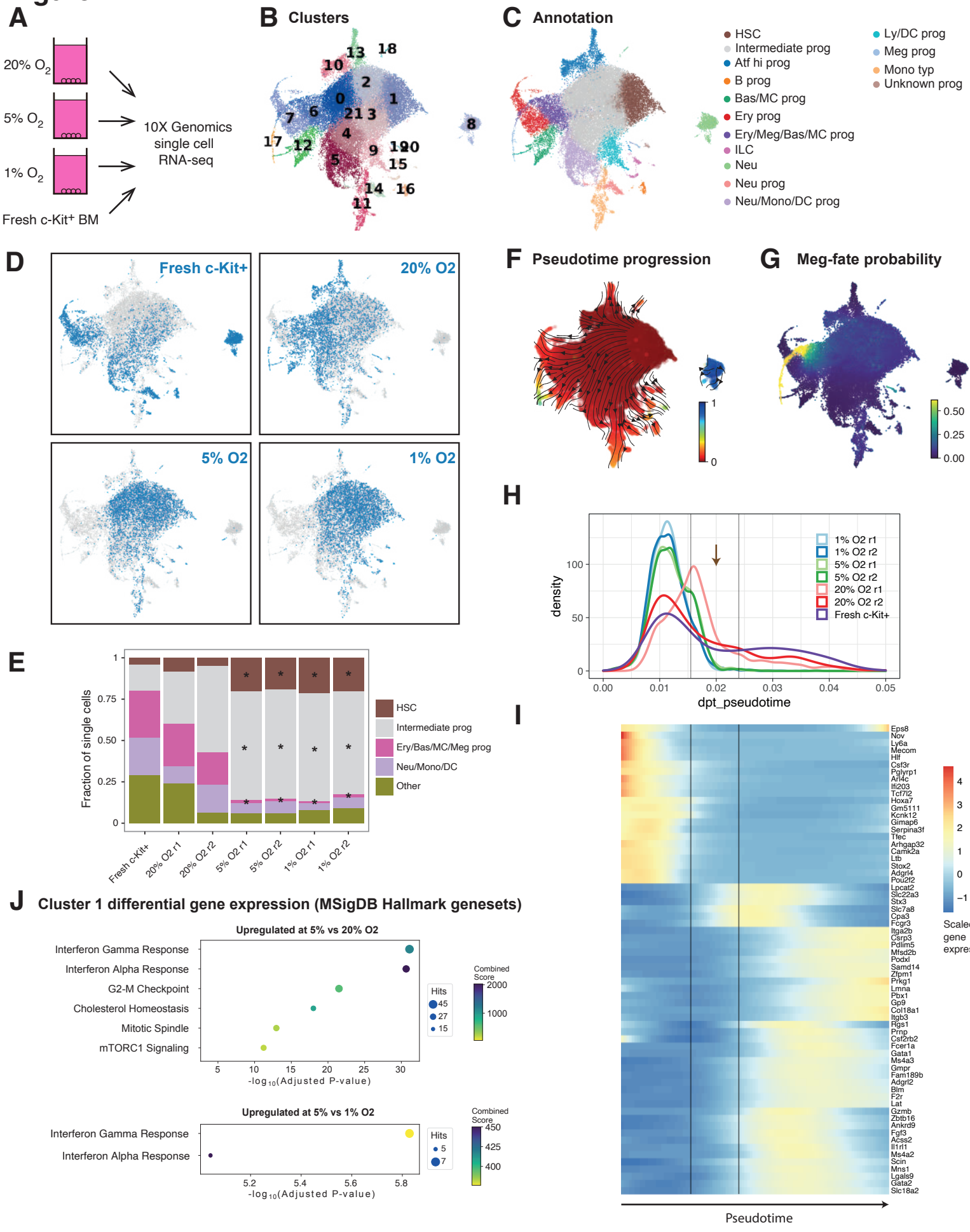

Figure 3

Figure 3

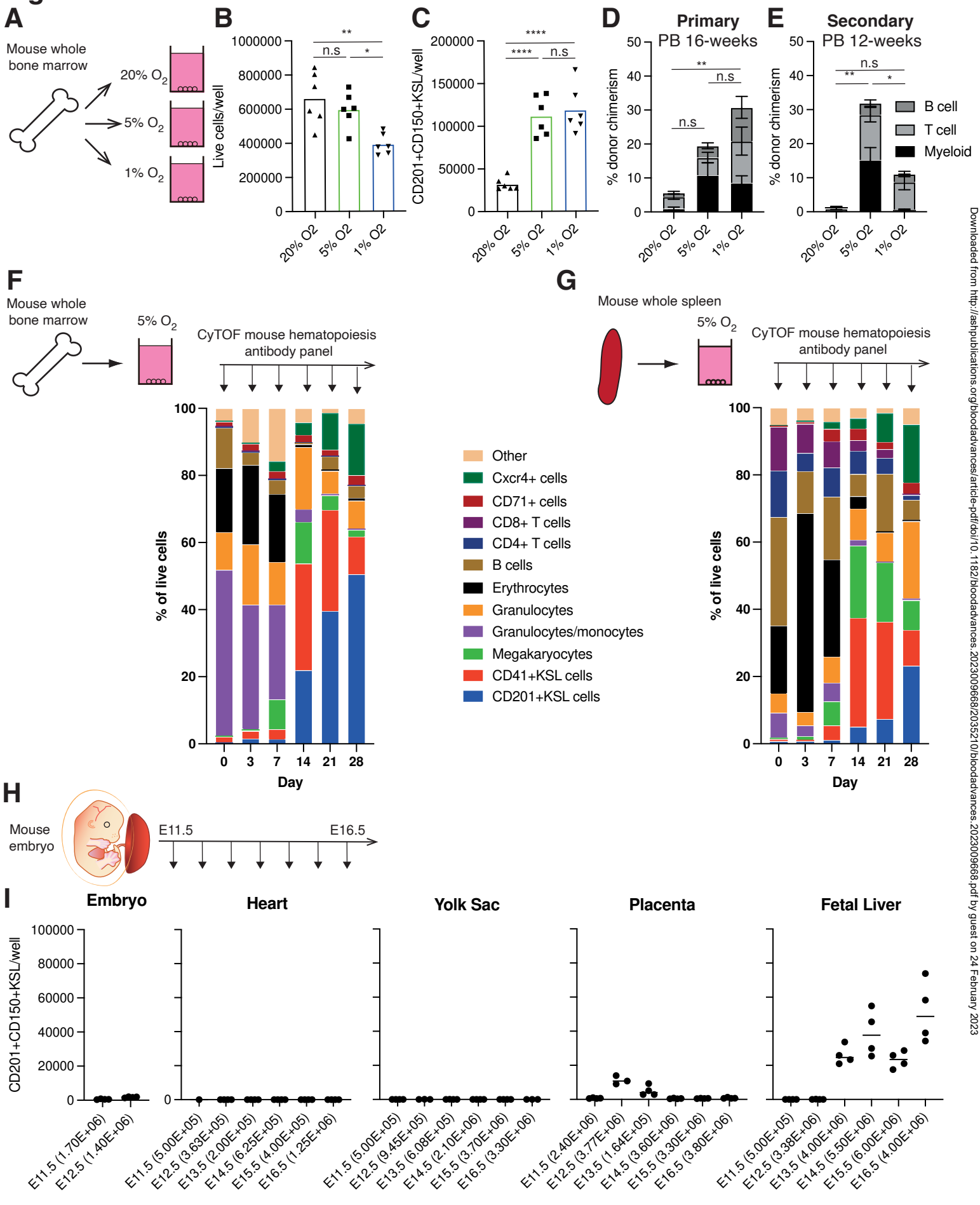

Figure 4